Prediction of the Intermittency Factor for Turbulent Shear Flows

W. Kollmann*
University of California, Davis, California

Two closure models for the prediction of the intermittency factor are discussed and their performance in free shear flows is evaluated. The first model is based on a closed set of conditional moment equations containing mean velocities in turbulent and nonturbulent zones and selected second-order moments in the turbulent zone. The second model is centered around the closed equation for the probability density function of a passive scalar which is suitable for discrimination between zones. The results show that the first model gives better agreement with measurements.

I. Introduction

TURBULENT shear flows with free boundaries show an intermittent character. The turbulent zone is separated from the nonturbulent zone by a highly fluctuating and sharp interface.[1] Conditional statistics[2] are required to describe this intermittent feature of turbulent shear flows. The intermittency factor plays a central role in this description because it contains the probability to encounter turbulent flow at a given point and links the unconditional to the zone-conditional moments (see Ref. 3, Appendix).

The earliest attempts to calculate the intermittency factor as solution of a closed-transport equation are due to Libby.[4,5] Dopazo[2] and Dopazo and O'Brien[6] developed the statistical formalism and evaluated the entrainment terms in conditional moment equations. A further modeled equation for the intermittency factor is due to Chevray and Tutu.[7] A complete closure model for the intermittency factor and conditional moments based on the k-ϵ model was presented in Ref. 3.

The alternative way of calculating the intermittency factor from the probability density function (pdf) of a scalar, which can serve as discriminator between turbulent and nonturbulent states of a flow, was discussed from the experimenter's point of view[8] but no predictions have been presented so far. This will be done in this paper. The pdf of a conserved passive scalar, such as small excess temperature, is considered and the closure model for the pdf-equation developed in Ref. 9 is applied to calculate the pdf and to extract from the result the intermittency factor. The calculations for both closure models are compared with experimental values to evaluate their properties.

II. Intermittency Factor and Conditional Moments

Characteristic functions defined by

$$I(\boldsymbol{x},t)=1 \quad \text{condition } A \text{ satisfied at } (\boldsymbol{x},t)$$

$$=0 \quad \text{otherwise}$$

where A is a noncontradictory condition which can be evaluated with quantities at the point $(\boldsymbol{x},t)$ only, lead to conditional moments. If A is the condition that the flow is turbulent at $(\boldsymbol{x},t)$ we obtain the statistics appropriate for turbulent shear flows with free boundaries (see Ref. 2 in particular). The condition for the flow to be turbulent involves, however, the variance of the vorticity fluctuations, which is difficult to measure. Therefore, other passive scalars (such as small excess temperature) are used to discriminate between the turbulent and nonturbulent states of the flow. The condition A is, then, as follows: the discriminating scalar $\Phi(\boldsymbol{x},t)$ is above a given threshold value.

The prediction of the intermittency factor $\gamma \equiv \langle I \rangle$ will be approached in two ways: the moment method and the pdf method. Each method has particular advantages and will be discussed briefly.

A. Moment Method

The exact moment equations up to second order for constant density flow can be derived by means of the characteristic function. The equation for the intermittency factor can be given as follows.

$$\frac{\partial \gamma}{\partial t}+\tilde{v}_\alpha \frac{\partial \gamma}{\partial x_\alpha}=\frac{\partial}{\partial x_\alpha}F_\alpha+S_\gamma \tag{1}$$

where the flux F_α is

$$F_\alpha \equiv \gamma(1-\gamma)(\tilde{\tilde{v}}_\alpha-\tilde{\tilde{v}}_\alpha) \tag{2}$$

and the entrainment S_γ is defined by

$$S_\gamma \equiv \langle V\delta(S)\rangle \tag{3}$$

The turbulent zone expectation of a random variable is denoted by

$$\tilde{\tilde{\phi}} \equiv \frac{\langle I\phi\rangle}{\gamma}, \qquad \phi=\tilde{\tilde{\phi}}+\phi^*$$

the nonturbulent zone expectation by

$$\tilde{\bar{\phi}} \equiv \frac{\langle (1-I)\phi\rangle}{1-\gamma}, \qquad \phi=\tilde{\bar{\phi}}+\phi^0$$

Unconditional expectations are denoted by $\bar{\phi}$ or $\langle\phi\rangle$.

The interface between the turbulent and the nonturbulent zones is determined implicitly by $S(\boldsymbol{x},t)=0$. The interface velocity v_α^S defines the relative progression velocity V by

$$n_\alpha V=v_\alpha-v_\alpha^S$$

Presented as Paper 83-0382 at the AIAA 21st Aerospace Sciences Meeting, Reno, Nev., Jan. 10-13, 1983; submitted Jan 29, 1983; revision submitted June 9, 1983.

*Associate Professor, Department of Mechanical Engineering.

where n is the normal vector of the interface positive into the turbulent zone.

The closure of the intermittency equation requires consideration of the entrainment S_γ. The model developed in Ref. 3 consists of three parts:

$$S_\gamma \cong S_\gamma^{(1)} + S_\gamma^{(2)} + S_\gamma^{(3)} \tag{4}$$

The part $S_\gamma^{(1)}$ describes the growth of the turbulent zone by entrainment of nonturbulent fluid due to production of kinetic energy of turbulence

$$S_\gamma^{(1)} \cong -C_1\gamma(1-\gamma)\frac{\widetilde{v_\alpha^* v_\beta^*}}{\tilde{\tilde{k}}}\frac{\partial \tilde{v}_\alpha}{\partial x_\beta} \tag{5}$$

The second part $S_\gamma^{(2)}$ reflects the enhanced convection of γ due to the fluctuations in the turbulent zone

$$S_\gamma^{(2)} \cong C_2\frac{\tilde{\tilde{k}}^2}{\tilde{\tilde{\epsilon}}}\frac{\partial\gamma}{\partial x_\alpha}\frac{\partial\gamma}{\partial x_\alpha} \tag{6}$$

The third part takes into account the dissipation of turbulent motion, which leads to reduction of enstrophy, thus diminishing γ.

$$S_\gamma^{(3)} \cong -C_3\gamma(1-\gamma)\frac{\tilde{\tilde{\epsilon}}}{\tilde{\tilde{k}}} \tag{7}$$

It should be noted that, in developed shear layers, the sum S_γ is positive nearly everywhere. If no shear is present, the intermittency factor decays as experiments[16] have shown. This requires the destructive contribution $S_\gamma^{(3)}$, if a finite threshold value for the discriminating scalar is assumed. For parabolic flows, the flux F_α is better represented by a model of the gradient-flux type than by direct calculation of the conditional cross-flow velocities.

$$F_\alpha \cong (1-\gamma)\frac{\tilde{\tilde{\nu}}_t}{\sigma_\gamma}\frac{\partial\gamma}{\partial x_\alpha} \tag{8}$$

where $\tilde{\tilde{\nu}}_t$ is the turbulent viscosity defined by

$$\tilde{\tilde{\nu}}_t = C_D\frac{\tilde{\tilde{k}}^2}{\tilde{\tilde{\epsilon}}} \tag{9}$$

The final equation for the intermittency factor γ for parabolic flows and a turbulence model based on the concept of turbulent pseudoviscosity[12] is, then,

$$\tilde{u}\frac{\partial\gamma}{\partial x}+\tilde{v}\frac{\partial\gamma}{\partial y}=\frac{\partial}{\partial y}\left[(1-\gamma)\frac{\tilde{\tilde{\nu}}_t}{\sigma_\gamma}\frac{\partial\gamma}{\partial y}\right]+C_1\gamma(1-\gamma)\frac{\tilde{\tilde{k}}}{\tilde{\tilde{\epsilon}}}\left(\frac{\partial\tilde{u}}{\partial y}\right)^2$$
$$+C_2\frac{\tilde{\tilde{k}}}{\tilde{\tilde{\epsilon}}}\left(\frac{\partial\gamma}{\partial y}\right)^2-C_3\gamma(1-\gamma)\frac{\tilde{\tilde{\epsilon}}}{\tilde{\tilde{k}}} \tag{10}$$

The complete closure model includes the equations for γ, the turbulent zone and nonturbulent zone mean velocities $\tilde{\tilde{u}}$ and $\tilde{u}$, the turbulent zone kinetic energy $\tilde{\tilde{k}}$, and the dissipation rate $\tilde{\tilde{\epsilon}}$. They are given in Appendix A together with the model constants.

B. The pdf Method

Consider a normalized bounded scalar $\Phi(x,t)$ which allows local discrimination between turbulent and nonturbulent states. Let Φ satisfy instantaneously

$$\frac{\partial\Phi}{\partial t}+v_\alpha\frac{\partial\Phi}{\partial x_\alpha}=\frac{\partial}{\partial x_\alpha}\left(\Gamma\frac{\partial\Phi}{\partial x_\alpha}\right)+S_\Phi \tag{11}$$

The pdf $P(\phi,x,t)$ of the values of ϕ of Φ at a given point (x,t) satisfies, then,[9]

$$\frac{\partial P}{\partial t}+\tilde{v}_\alpha\frac{\partial P}{\partial x_\alpha}=\frac{\partial}{\partial x_\alpha}\left[\Gamma\frac{\partial P}{\partial x_\alpha}-\langle v'_\alpha\hat{P}\rangle\right]$$
$$-\frac{\partial^2}{\partial\phi^2}\langle\Gamma\nabla\Phi\cdot\nabla\Phi\hat{P}\rangle-\frac{\partial}{\partial\phi}\langle S\hat{P}\rangle \tag{12}$$

where $\hat{P}\equiv\delta(\Phi(x,t)-\phi)$. The pdf P is split into

$$P(\phi)=p_1\delta(\phi)+p_2\delta(1-\phi)+(1-p_1-p_2)P_c(\phi) \tag{13}$$

where $P_c(\phi)$ is the continuous part of P and p_1,p_2 the amplitudes of the singular parts at the end points of the unit interval.

The intermittency factor γ follows from Eq. (13) as

$$\gamma=1-\left(p_1+\int_{+0}^{\delta}d\phi P_c(\phi)\right)-\left(p_2+\int_{1-\delta}^{1-}d\phi P_c(\phi)\right) \tag{14}$$

Integration of Eq. (12) over the intervals $[0,\delta]$ and $[1-\delta,1]$ yields the equations for p_1 and p_2.[9]

$$\frac{\partial p_i}{\partial t}+\tilde{v}_\alpha\frac{\partial p_i}{\partial x_\alpha}=\frac{\partial}{\partial x_\alpha}F_\alpha^{(i)}-S_i,\qquad i=1,2 \tag{15}$$

where

$$F_\alpha^{(1)}=p_1(1-p_1)[\langle v_\alpha/\Phi\geq 1-\delta\rangle-\langle v_\alpha/\Phi\leq\epsilon\rangle]$$
$$+(1-p_1-p_2)p_1[\langle v_\alpha/\delta<\Phi<1-\delta\rangle-\langle v_\alpha/\Phi\geq 1-\delta\rangle] \tag{16}$$

and

$$F_\alpha^{(2)}=p_2(1-p_2)[\langle v_\alpha/\Phi\leq\delta\rangle-\langle v_\alpha/\Phi\geq 1-\delta\rangle]$$
$$+(1-p_1-p_2)p_2[\langle v_\alpha/\delta<\Phi<1-\delta\rangle-\langle v_\alpha/\Phi\leq\delta\rangle] \tag{17}$$

The source terms S_i can be related to the scalar dissipation and S_Φ by

$$S_1=\frac{\partial}{\partial\phi}\langle\Gamma\nabla\Phi\cdot\nabla\Phi\hat{P}\rangle|_{\phi=\delta}+S_\Phi(\delta)+O(\delta)$$

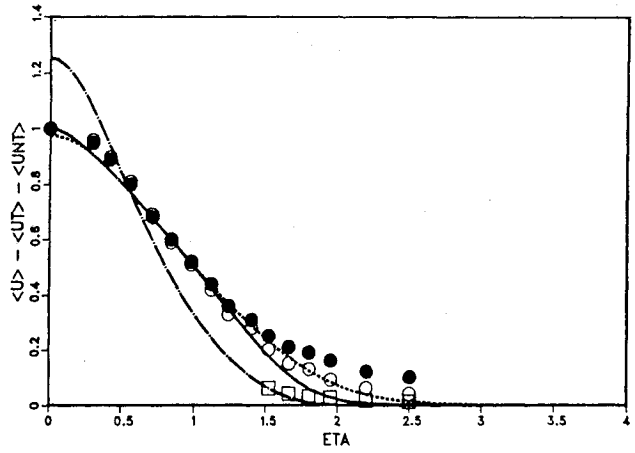

Fig. 1 Mean velocity profiles for plane jet (conditional model, experiment of Ref. 13). For the unconditional mean, the full line is prediction and the open circles are the experiment. For the turbulent zone mean, the broken line is prediction and the full circles are the experiment. For the nonturbulent zone mean, the dashpot line is prediction and the open rectangles are the experiment.

and

$$S_2 = -\frac{\partial}{\partial\phi}\langle\Gamma\nabla\Phi\cdot\nabla\Phi\hat{P}\rangle|_{\phi=1-\delta} + S_\Phi(1-\delta) + 0(\delta)$$

where $0(\delta)$ indicates terms vanishing with $\delta\to 0$.

It should be noted that two "nonturbulent" zones can be distinguished here with values $\phi=0$ or $\phi=1$ of the discriminating scalar Φ. This situation would occur if excess temperature is used in a flow with a nonturbulent warm and a nonturbulent cold boundary (mixing layer). The closure of Eqs. (12) and (15) in the context of a two-turbulence model was developed and tested in several shear flows.[9] The resulting modeled equations are given by

$$\frac{\partial P}{\partial t} + \langle v_\alpha\rangle\frac{\partial P}{\partial x_\alpha} = \frac{\partial}{\partial x_\alpha}\left(\Gamma + \frac{\nu_t}{\sigma_p}\right)\frac{\partial P}{\partial x_\alpha} + \frac{C_c}{\tau_c}(1-p_1-p_2)$$
$$\times\left[\int_0^\phi d\phi'\int_\phi^1 d\phi'' P_c(\phi')P_c(\phi'')R(\phi',\phi'',\phi) - P_c(\phi)\right]$$
$$+\frac{C_a}{\tau}(1-p_1-p_2)[p_1P_{d_1}(\phi)+p_2P_{d_2}(1-\phi)]$$
$$+\frac{C_a}{\tau}(1-p_1-p_2)\frac{\phi-\langle\Phi\rangle_c}{\langle\Phi'^2\rangle_c}P_c(\phi)$$
$$\times\left[p_1\int_0^1 d\phi'\phi' P_{d_1}(\phi') - p_2\int_0^1 d\phi'\phi' P_{d_2}(\phi')\right]$$
$$+\frac{C_a}{\tau}[p_1p_2P_d(\phi)+p_1p_2P_d(1-\phi)] \qquad (18)$$

and

$$\frac{\partial p_i}{\partial t} + \langle v_\alpha\rangle\frac{\partial p_i}{\partial x_\alpha} = \frac{\partial}{\partial x_\alpha}\left[\left(\Gamma+\frac{\nu_t}{\sigma_p}\right)\frac{\partial p_i}{\partial x_\alpha}\right] - \frac{C_a}{\tau}p_i(1-p_i) \quad i=1,2 \qquad (19)$$

The function $R(\phi',\phi'',\phi)$ is defined as

$$R(\phi',\phi'',\phi) = 2/(\phi''-\phi') \quad \text{for } 0\le\phi'\le\phi\le\phi''\le 1$$
$$= 0 \quad \text{otherwise}$$

The time scales are

$$\tau^{-1} = \frac{\epsilon}{k}, \qquad \tau_c^{-1} = \frac{\epsilon}{k}\left(0.4\ln\frac{\overline{T'}}{\Delta T_0} + 3.05\right)$$

where τ_c^{-1} was modified on the basis of measurements of Warhaft and Lumley[10] [$T' = (\overline{T'^2})^{1/2}$ and ΔT_0 is the difference of jet pipe exit and ambient temperatures]. The function P_d (and P_{d1}, P_{d2}), which describes the entrainment of nonturbulent fluid into the turbulent zone in terms of the interaction of the singular parts with each other and the continuous part, is constructed as power function (P_{d1}, P_{ds} are the same form with ϕ_{s1}, ϕ_{s2})

$$P_d(\phi) = 1/\phi_s(1+e)(1-\phi/\phi_s)^e \quad \text{for } 0\le\phi\le\phi_s$$
$$= 0 \quad \text{otherwise}$$

and $e = 1 + C_e(k^2/\epsilon\Gamma)^\alpha$. This corresponds to the variation of ϕ as power of the normal distance through the interface. Note that subscript c denotes moments of $P_c(\phi)$. The additional equations of the k-ϵ model are given in Appendix B together with the model constants.

III. Applications

The conditional turbulence model and the closure model for the scalar pdf were applied to plane shear flows to compare and evaluate their ability to predict the intermittency factor and other moments. A standard finite difference procedure[11] was applied to the numerical solution of the system of parabolic differential equations. The additional independent variable in the pdf-model described in Section II.B does not pose any new problems for the solution because the modeled Eq. (18) does not contain derivatives with respect to this axis. The number of grid points in the cross-flow direction was $N_1 = 100$ for the conditional model and $N_2 = 60$ for the pdf model, which was discretized in $M = 30$ points in the scalar direction.

A. Plane Jet

Both prediction models were applied to the plane jet configuration of Ref. 13. The initial conditions were rectangular profiles for mean velocities and temperature $T^* = (T-T_\infty)/(T_0-T_\infty)$ in the case of the pdf model. This implies that the pdf of T^* at the entrance is given by a rectangular profile for p_1 with $P_c = 0$ and $p_2 = 1-p_1$. The initial intermittency factor is $\gamma_0 = 0.01$ and constant across the entrance section. The initial kinetic energy is small ($k = 10^{-5}$ m^2/s^2) and the initial dissipation rate is determined from the equilibrium condition for k. The boundary conditions are the standard zero gradient at the symmetry axis and Dirichlet conditions at the outer edge. A small velocity u_∞ ($u_\infty = u_0/34$) was chosen at the outer edge to avoid numerical difficulties. The results (at $x/D = 40$) are shown in Figs. 1-7. The predicted spreading rates

$$\frac{dy_{0.5}}{dx} = 0.116 \text{ for conditional model}$$
$$= 0.109 \text{ for pdf-model}$$

agree well with the experimental value of $dy_{0.5}/dx \cong 0.11$ as given by Rodi.[15] The mean velocity profiles ($\eta \equiv y/y_{0.5}$, normalized with unconditional mean values) for the conditional model show good agreement with the experiments.[13] It is worth noting that the nonturbulent zone velocity has a higher value at the axis and smaller half width. The movement of the interface supplies the energy for the fluctuations in the nonturbulent zone. The closed equation (A2) reflects this property in terms of a diffusivity proportional to the intermittency factor. The calculation was started with a nonturbulent flow and, therefore, attains the nonturbulent zone profile higher axial values than the turbulent zone profile. The

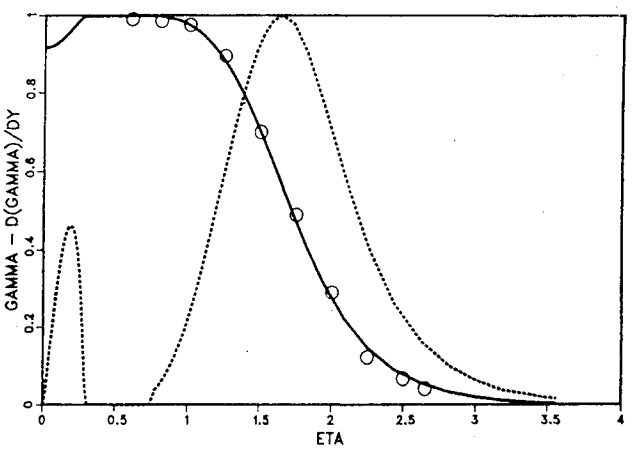

Fig. 2 Intermittency factor for plane jet (conditional model, experiment of Ref. 13). The full line is prediction and the symbols are the experiment; the broken line is $|d\gamma/dy|$ from the predicted curve.

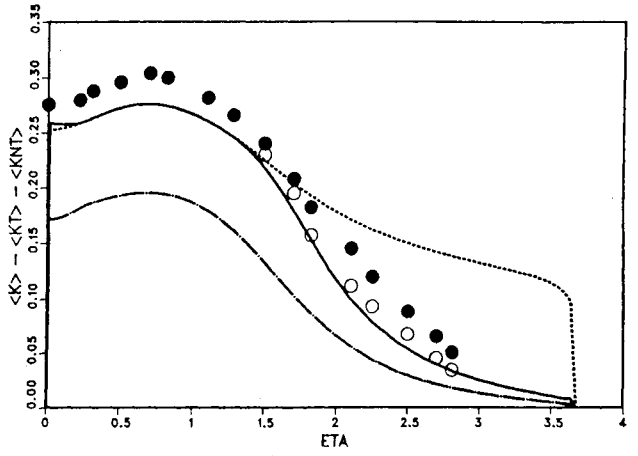

Fig. 3 Comparison of predicted (conditional model, experiment of Ref. 13) turbulence intensities with experimental $u'/\tilde{u}_0$. For legend see Fig. 1.

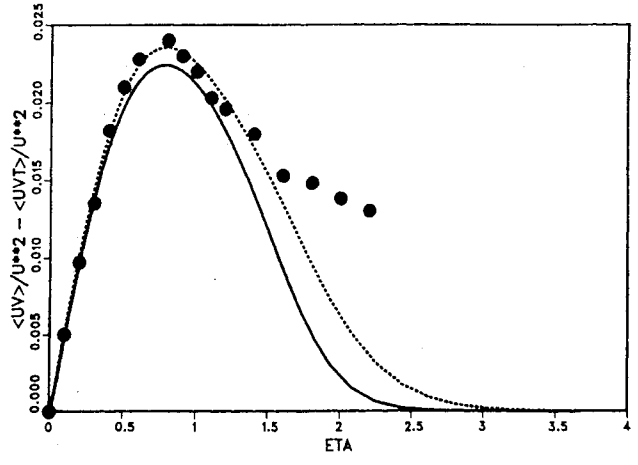

Fig. 4 Comparison of predicted (conditional model, experiment of Ref. 13) shear stress with experiment. For legend see Fig. 1.

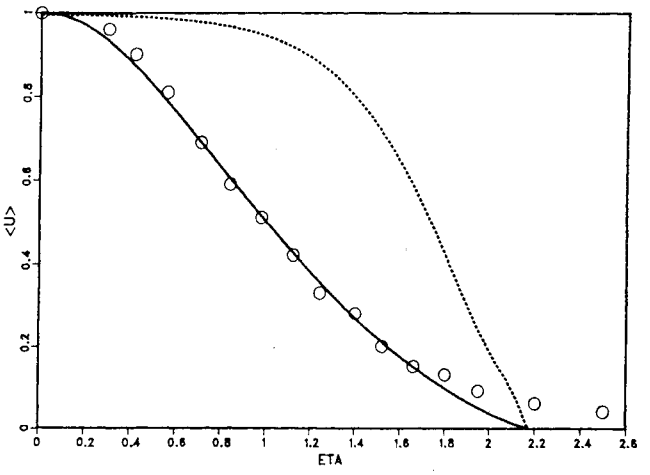

Fig. 5 Unconditional mean velocity for plane jet (pdf model) the full line is prediction and the open circles are experiment of Ref. 13; the broken line is the predicted intermittency factor.

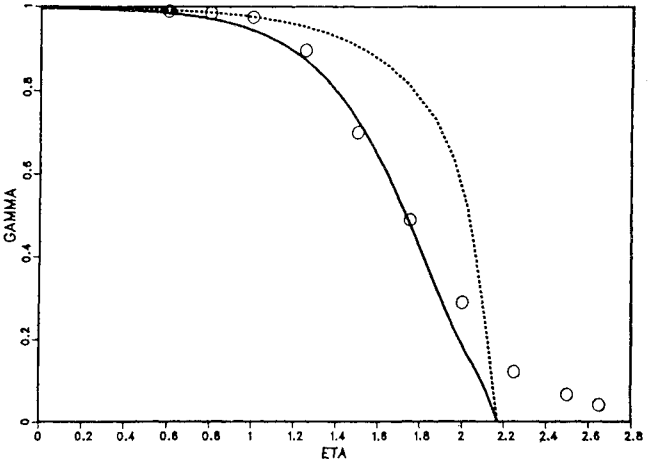

Fig. 6 Intermittency factor γ (pdf model, Eq. (14), full line) and $1-p_1-p_2$ (broken line) compared with expriment of Ref. 13.

intermittency factor γ in Fig. 2 agrees with the measurements of Ref. 13 but shows a remnant of the initially nonturbulent core as a slight dip near the axis. This dip vanishes slowly downstream due to the factor $(1-\gamma)$ of the diffusivity in Eq. (10). The broken line is $|d\gamma/dy|$ as a measure for the crossing frequency of the interface. The kinetic energies $k, \tilde{k}, \bar{\tilde{k}}$ in Fig. 3 and the shear stresses $u'v', \widetilde{u^*v^*}$ in Fig. 4 calculated from the mean profile (see Ref. 3) are compared with u'/u_0 and $u'v'/u_0^2$, respectively, of Ref. 13 showing reasonable agreement. The properties of the pdf model can be evaluated from Figs. 5-7. As a check, the unconditional mean velocity in Fig. 5 shows that the overall properties of the plane jet are well predicted. The intermittency factor was calculated according to Eq. (14) with a threshold value of $\delta=0.23$ K for $T_0-T_\infty=20$ K excess temperature. The γ profile in Fig. 6 agrees well with the experiment in Ref. 13 in the main part of the flow but falls off too rapidly at the outer edge. This is due to the fact that the pdf model is based solely on unconditional quantities. The pdf for T^* in Fig. 7 shows the characteristic bimodal form (for details see Ref. 9).

B. Plane Shear Layer

The initial and boundary conditions for the shear layer are the same as for the jet except that both boundaries have Dirichlet conditions. The values for the outer velocities were chosen to simulate the experiments of Ref. 14. The predicted spreading rate

$$\frac{d}{dx}(y_{0.1}-y_{0.9}) = 0.12 \text{ for conditional model}$$

$$= 0.14 \text{ for pdf model}$$

are on the low side of the experimental values which vary from 0.13-0.2 (Ref. 15). The mean velocities for the conditional model [$\eta \equiv (y-y_{0.5})/(y_{0.1}-y_{0.9})$, normalized with boundary values] show good agreement for the unconditional mean in Fig. 8 except at the high-speed side where the predicted curve is too steep. The turbulent zone mean in Fig. 9 agrees well with the experiment. The departure at the low-speed side is mostly due to the normalization of the predictions, which are compared with $\tilde{u}/u_m$ of the experiments, which have a nonzero velocity at the low-speed side. The nonturbulent zone mean in Fig. 10 agrees remarkably well with the expriments, thus confirming the closure suggested in Eq. (A2). The intermittency factor in Fig. 11 shows the same shape as the experiments but is too broad and shifted to the low-speed side. There are two reasons for this. The high-speed side of the mean velocity profile is too steep, thus making $y_{0.1}-y_{0.9}$ too small and, therefore, profiles plotted against the nondimensional coordinate appear broader. The shear layer is known to contain large-scale structures with long life-time, which lead to a more intermittent character of the flow than

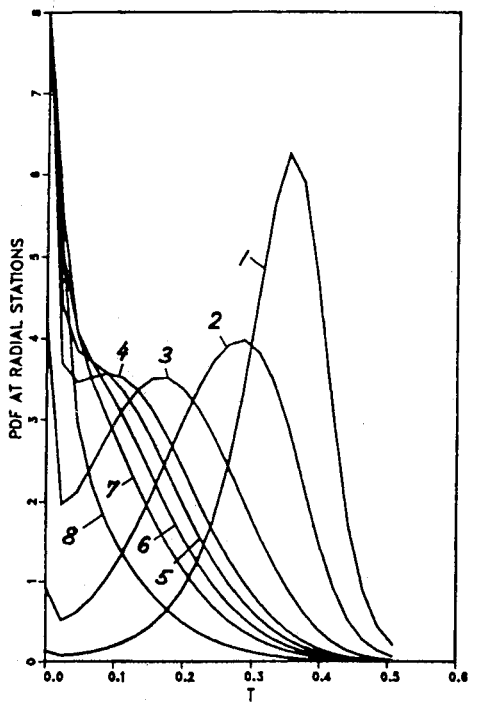

Fig. 7 pdf of bounded passive scalar at several y-stations: 1) $\eta = 0.0$; 2) $\eta = 0.68$; 3) $\eta = 1.1$; 4) $\eta = 1.34$; 5) $\eta = 1.43$; 6) $\eta = 1.52$; 7) $\eta = 1.61$; 8) $\eta = 1.82$.

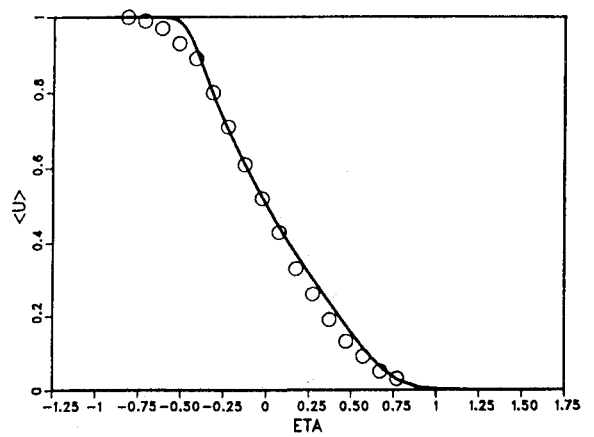

Fig. 8 Unconditional mean velocity in plane shear layer (conditional model). The full line is prediction and the symbols are experiment of Ref. 14.

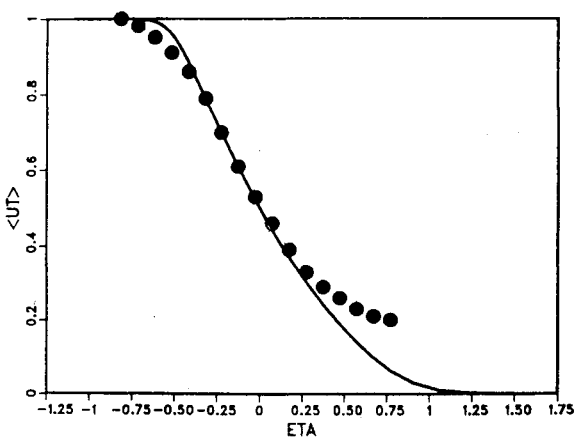

Fig. 9 Turbulent zone mean velocity in plane shear layer (conditional model). The full line is prediction and the symbols are experiment of Ref. 14.

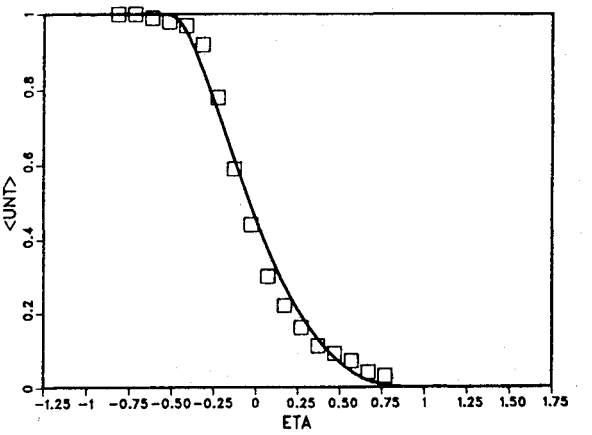

Fig. 10 Nonturbulent zone mean velocity in plane shear layer (conditional model). The full line is prediction and the symbols are experiment of Ref. 14.

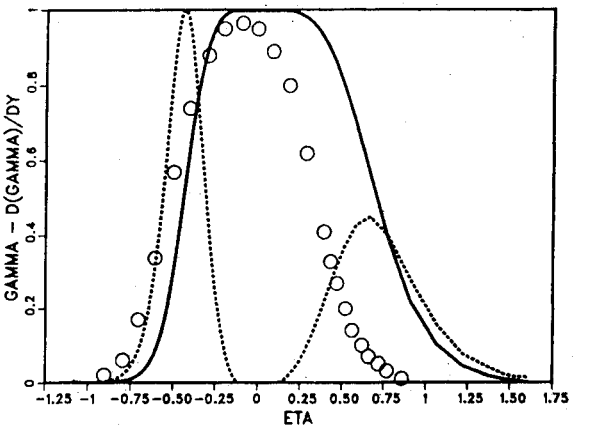

Fig. 11 Intermittency factor for plane shear layer (conditional model, experiment of Ref. 14). For legend see Fig. 2.

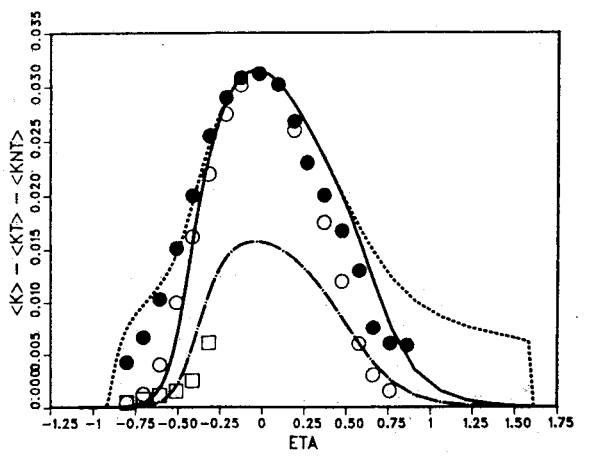

Fig. 12 Comparison of predicted (conditional model, experiment of Ref. 14) turbulence intensities with experimental $u'/\tilde{u}_0$. For legend see Fig. 1.

the prediction model simulates. The kinetic energies in Fig. 12 compared with the longitudinal fluctuations of Ref. 14 show good agreement for all zones. The pdf model in Figs. 13-15 confirms the properties already shown in case of the jet. The intermittency factor in Fig. 13 is too broad and falls off too rapidly at the edges. The mean velocity in Fig. 14 shows the same deviation at the high-speed side as the conditional model. Finally, the pdf in Fig. 15 again has a bimodal form quite different from the Gaussian form.

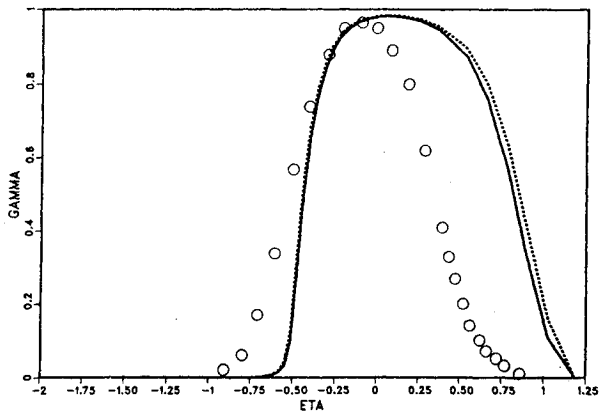

Fig. 13 Intermittency factor γ for plane shear layer (pdf model, equation (14), full line) and $1-p_1-p_2$ (broken line) compared with experiment of Ref. 14.

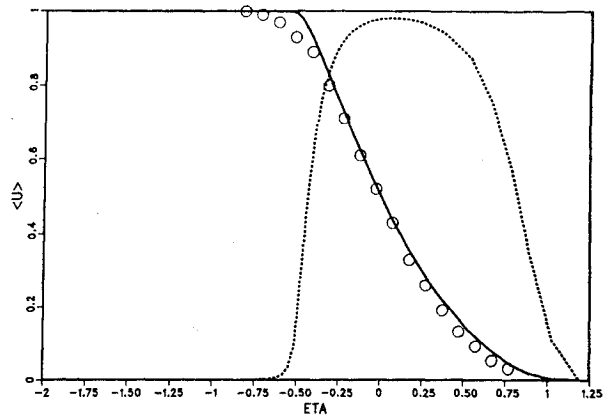

Fig. 14 Unconditional mean velocity for plane shear layer (pdf model); the full line is prediction and the symbols are experiment of Ref. 14; the broken line is the predicted intermittency factor.

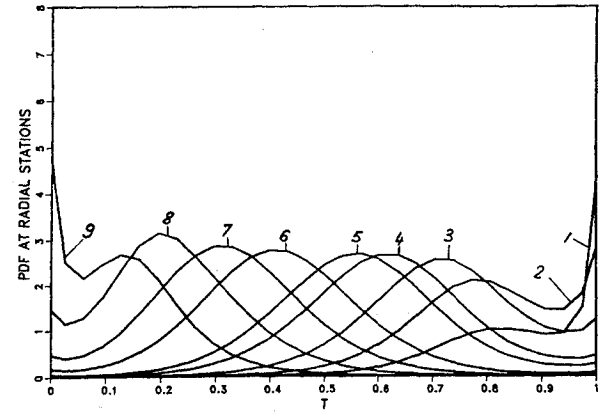

Fig. 15 pdf of bounded passive scalar at several y stations: 1) $\eta=-0.46$; 2) $\eta=-0.376$; 3) $\eta=-0.276$; 4) $\eta=-0.14$; 5) $\eta=-0.067$; 6) $\eta=0.143$; 7) $\eta=0.3$; 8) $\eta=0.5$; 9) $\eta=0.73$.

IV. Conclusions

The comparison of the conditional and the pdf models with experiments for plane jet and plane mixing layer leads to several conclusions.

1) The intermittently turbulent free boundary of turbulent shear layers is better described by the conditional closure model than by the pdf model because the conditional moments are determined in this region by the interface term, whereas the intermittency factor calculated from the pdf of a passive scalar is determined by unconditional quantities and does not influence the momentum transport. The pdf model in the present context is, therefore, less sophisticated than the moment model. If the velocity is included as independent variable, the pdf provides a more complete description of the flowfield and can be expected to be superior.

2) Calculation of the intermittency factor from the pdf of a passive scalar gives reasonable results in the main part of the flow provided the threshold value for the discriminating scalar is known.

3) Further improvement of these models should be aimed at the dissipation rate equation, which determines length and time scales.

Appendix A

The complete moment model for the prediction of the intermittency factor γ includes, in addition to Eq. (10), the following equations (parabolic plane flows).

Turbulent zone mean velocity $\bar{\tilde{u}}$

$$\bar{u}\frac{\partial\bar{\tilde{u}}}{\partial x}+\bar{v}\frac{\partial\bar{\tilde{u}}}{\partial y}=\frac{\partial}{\partial y}\left[(\nu+\bar{\tilde{\nu}}_t)\frac{\partial\bar{\tilde{u}}}{\partial y}\right]-\frac{1}{\rho}\frac{\partial\bar{\tilde{p}}}{\partial x}+(C_{m1}-\gamma)\frac{\bar{\tilde{\nu}}_t}{\gamma}\frac{\partial\gamma}{\partial y}\frac{\partial\bar{\tilde{u}}}{\partial y} \tag{A1}$$

Nonturbulent zone mean velocity $\bar{\tilde{u}}$

$$\bar{u}\frac{\partial\bar{\tilde{u}}}{\partial x}+\bar{v}\frac{\partial\bar{\tilde{u}}}{\partial y}=\frac{\partial}{\partial y}\left[(\nu+C_4\gamma\bar{\tilde{\nu}}_t)\frac{\partial\bar{\tilde{u}}}{\partial y}\right]-\frac{1}{\rho}\frac{\partial\bar{\tilde{p}}}{\partial x} \tag{A2}$$

Turbulent zone kinetic energy $\bar{\tilde{k}}$

$$\bar{u}\frac{\partial\bar{\tilde{k}}}{\partial x}+\bar{v}\frac{\partial\bar{\tilde{k}}}{\partial y}=\frac{\partial}{\partial y}\left[\left(\nu+\frac{\bar{\tilde{\nu}}_t}{\sigma_k}\right)\frac{\partial\bar{\tilde{k}}}{\partial y}\right]+\bar{\tilde{\nu}}_t\left(\frac{\partial\bar{\tilde{u}}}{\partial y}\right)^2-\bar{\tilde{\epsilon}}+F_k \tag{A3}$$

The interface terms are collected in F_k

$$F_k\equiv\left(\frac{1}{\sigma_k}+\frac{1-\gamma}{\sigma_\gamma}\right)\frac{\bar{\tilde{\nu}}_t}{\gamma}\frac{\partial\gamma}{\partial y}\frac{\partial\bar{\tilde{k}}}{\partial y}+\frac{\bar{\tilde{k}}}{\gamma}\left[\nu\frac{\partial^2\gamma}{\partial y^2}-S_\gamma\right]+C_{k1}(1-\gamma)\bar{\tilde{\epsilon}} \tag{A4}$$

Dissipation rate $\bar{\tilde{\epsilon}}$

$$\bar{u}\frac{\partial\bar{\tilde{\epsilon}}}{\partial x}+\bar{v}\frac{\partial\bar{\tilde{\epsilon}}}{\partial y}=\frac{\partial}{\partial y}\left[\left(\nu+\frac{\bar{\tilde{\nu}}_t}{\sigma_\epsilon}\right)\frac{\partial\bar{\tilde{\epsilon}}}{\partial y}\right]+C_{\epsilon1}C_D\bar{\tilde{k}}\left(\frac{\partial\bar{\tilde{u}}}{\partial y}\right)^2-C_{\epsilon2}\frac{\bar{\tilde{\epsilon}}^2}{\bar{\tilde{k}}}+F_\epsilon \tag{A5}$$

Interface terms

$$F_\epsilon\equiv\left(\frac{1}{\sigma_\epsilon}+\frac{1-\gamma}{\sigma_\gamma}\right)\frac{\bar{\tilde{\nu}}_t}{\gamma}\frac{\partial\gamma}{\partial y}\frac{\partial\bar{\tilde{\epsilon}}}{\partial y}+\frac{\bar{\tilde{\epsilon}}}{\gamma}\left(\nu\frac{\partial^2\gamma}{\partial y^2}-S_\gamma\right)+C_{\epsilon3}(1-\gamma)\frac{\bar{\tilde{\epsilon}}^2}{\bar{\tilde{k}}} \tag{A6}$$

Note that for the entrainment S_γ, the model in Eq. (10) has to be inserted. The model constants are as follows: $C_1=0.2$; $C_2=0.6$; $C_3=0.1$; $C_4=0.5$; $C_{m1}=0.7$; $C_{k1}=2.5$; $C_D=0.09$; $C_{\epsilon1}=1.44$; $C_{\epsilon2}=1.95$; $C_{\epsilon3}=2.5$; $\sigma_\gamma=1.0$; $\sigma_k=1.0$; $\sigma_\epsilon=1.3$.

Appendix B

The additional equations for the pdf model for plane parabolic flows are given by[12]

$$\bar{u}\frac{\partial\bar{u}}{\partial x}+\bar{v}\frac{\partial\bar{u}}{\partial y}=\frac{\partial}{\partial y}\left[(\nu+\nu_t)\frac{\partial\bar{u}}{\partial y}\right]-\frac{1}{\rho}\frac{\partial\bar{p}}{\partial x}$$

and

$$\bar{u}\frac{\partial k}{\partial x}+\bar{v}\frac{\partial k}{\partial y}=\frac{\partial}{\partial y}\left[\left(\nu+\frac{\nu_t}{\sigma_k}\right)\frac{\partial k}{\partial y}\right]+\nu_t\left(\frac{\partial \bar{u}}{\partial y}\right)^2-\epsilon$$

and

$$\bar{u}\frac{\partial \epsilon}{\partial x}+\bar{v}\frac{\partial \epsilon}{\partial y}=\frac{\partial}{\partial y}\left[\left(\nu+\frac{\nu_t}{\sigma_k}\right)\frac{\partial \epsilon}{\partial y}\right]+C_{\epsilon 1}\nu_t\left(\frac{\partial \bar{u}}{\partial y}\right)^2-C_{\epsilon 2}\frac{\epsilon^2}{k}$$

The turbulent viscosity is defined as

$$\nu_t=C_D\frac{k^2}{\epsilon}$$

The model constants are: $C_a=3.0$; $C_c=3.2$; $C_e=0.5$; $\phi_s^\circ=0.3$; $\alpha=0.25$; $\sigma_P=0.7$. The values for the basic k-ϵ model[12] are the same as in Appendix A.

Acknowledgments

The author was supported by DOE Grant A S03-76SF00034. The work was done at the Combustion Research Facility of Sandia National Laboratory in Livermore.

References

[1]Corrsin, S. and Kistler, A. L., "The Free-Stream Boundaries of Turbulent Flows," NACA TN-3133, 1954.

[2]Dopazo, C., "On Conditional Averages for Intermittent Turbulent Flows," *Journal of Fluid Mechanics*, Vol. 81, Pt. 3, 1977, pp. 433-438.

[3]Byggstoyl, S. and Kollmann, W., "Closure Model for Intermittent Turbulent Flows," *International Journal of Mass Transfer*, Vol. 24, 1981, pp. 1811-1822.

[4]Libby, P. A., "On the Prediction of Intermittent Turbulent Flows," *Journal of Fluid Mechanics*, Vol. 68, 1975, pp. 273-295.

[5]Libby, P. A., "Prediction of the Intermittent Turbulent Wake of a Heated Cylinder," *Physics of Fluids*, Vol. 19, 1976, pp. 494-501.

[6]Dopazo, C. and O'Brien, E. E., "Intermittency in Free Turbulent Shear Flows," *Proceedings of the First Symposium on Turbulent Shear Flows*, Pennsylvania State Univ., 1977.

[7]Chevray, R. and Tutu, N. K., "Intermittency and Preferential Transport of Heat in a Round Jet," *Journal of Fluid Mechanics*, Vol. 88, 1978, pp. 133-160.

[8]Bilger, R. W., Antonia, R. A., and Sreenivasan, K. R., "Determination of Intermittency from the Probability Density Function of a Passive Scalar," *Physics of Fluids*, Vol. 19, 1976, pp. 1471-1474.

[9]Kollmann, W. and Janicka, J., "The Probability Density Function of a Passive Scalar in Turbulent Shear Flows," *Physics of Fluids*, Vol. 25, 1982, pp. 1755-1769.

[10]Warhaft, Z. and Lumley, J. L., "An Experimental Study of the Decay of Temperature Fluctuating in Grid Generated Turbulence," *Journal of Fluid Mechanics*, Vol. 88, 1978, pp. 659-684.

[11]Patankar, S. V. and Spalding, D. B., *Heat and Mass Transfer in Boundary Layers*, Intertext, London, 1970.

[12]Jones, W. P. and Launder, B. E., "The Prediction of Laminarization with a Two-Equation Model of Turbulence," *International Journal of Heat and Mass Transfer*, Vol. 15, 1972, pp. 301-314.

[13]Gutmark, E. and Wygnanski, I., "The Planar Turbulent Jet," *Journal of Fluid Mechanics*, Vol. 73, 1976, pp. 465-495.

[14]Wygnanski, I. and Fiedler, H. E., "The Two-Dimensional Mixing Region," *Journal of Fluid Mechanics*, Vol. 41, 1970, pp. 327-361.

[15]Rodi, W., "A Review of Experimental Data," *Studies of Convection*, edited by B. E. Launder, Vol. 1, Academic Press, New York, 1975, pp. 79-165.

[16]Mobbs, F. R., "Spreading and Contraction at the Boundaries of Free Turbulent Flows," *Journal of Fluid Mechanics*, Vol. 33, 1968, pp. 227-239.